

We are IntechOpen, the world's leading publisher of Open Access books Built by scientists, for scientists

6,900

Open access books available

185,000

International authors and editors

200M

Downloads

Our authors are among the

154

Countries delivered to

TOP 1%

most cited scientists

12.2%

Contributors from top 500 universities



WEB OF SCIENCE™

Selection of our books indexed in the Book Citation Index
in Web of Science™ Core Collection (BKCI)

Interested in publishing with us?
Contact book.department@intechopen.com

Numbers displayed above are based on latest data collected.
For more information visit www.intechopen.com



Modelling, Simulation and Dosimetry of ^{103}Pd Eye Plaque Brachytherapy

Pooneh Saidi and Mahdi Sadeghi

Abstract

In this study, the dose distribution has been calculated for the Collaborative Ocular Melanoma Study (COMS) eye plaques at various diameters 10–22 mm, loaded with the ^{103}Pd brachytherapy seeds (Model IR06- ^{103}Pd). Several Monte Carlo (MC) simulations have been employed to carry out the gold backing and Silastic insert effect on dose distribution around the eye plaque. Version 5 of the Monte Carlo N-particle (MCNP) code has been used to carry out the simulations. The new palladium seed was modelled in three geometric orientations (ideal, vertical and diagonal). Results are compared with the calculated data for COMS eye plaque loaded with Theragenics model 200 and Best model 2335 palladium-103 seeds and model 6711 iodine-125 seeds. The calculated dose rate constant of the IR06- ^{103}Pd seed was found to be $0.692 \pm 0.020 \text{ cGy h}^{-1} \text{ U}^{-1}$. The air kerma strength to deliver 85 Gy to tumour apex in a water medium was found to be 4.10 U/seed. The dosimetric parameters calculated in this work for the new palladium seed indicate the IR06- ^{103}Pd seed is suitable for use in brachytherapy. In COMS plaques, the dose distribution to points of interest was compared for three ^{103}Pd seed models. With the exception of sclera dose and for a given prescription dose, the IR06 seed delivers lower dose ocular points of interest.

Keywords: eye plaque, palladium-103, brachytherapy, dosimetry

1. Introduction

The most common primary intraocular malignancy in adults is choroidal melanoma, accounting for 5% of all melanomas, originating within the pigmented cells of the choroid. More common in Caucasians, the Collaborative Ocular Melanoma Study (COMS) found the mean age at diagnosis to be 60 years. Generally, they are located posterior to the ciliary body and often found during ophthalmic examination [1, 2].

The plaque is temporarily sutured to the sclera overlying the tumour, left in place for 5–7 days and then surgically removed. Temporary placement of an episcleral plaque containing radioactive material has gained acceptance as a treatment for choroidal melanoma. Compared to enucleation, eye plaque brachytherapy provides better outcomes for uveal melanoma [3]. The choice of the treatment

method is depending on the size and location of the tumour [4, 5]. One of the most common primary intraocular malignancies is the choroidal. Patients with a medium-sized choroidal melanoma (between 2.5 and 10 mm in height and <16 mm basal diameter) are candidates for episcleral plaques [6]. It offers good chances of conserving the eye, often with at least some useful vision [7, 8]. Compared to charged particle radiation, the collimating effects of an eye plaque provides better conformality than possible with protons and essentially zero dose to the brain and orbit behind the plaque. Different types of eye plaque are used for the treatment of intraocular tumours, which are most often round, made of gold, silver, or stainless steel and come in several diameters depending on the tumour size. The Collaborative Ocular Melanoma Study group provided the first standardized methods for administering ocular brachytherapy treatments for uveal melanoma in 1985, by the eye plaques, and for the brachytherapy seeds, the dose was calculated using a point source approximation, and no corrections were made for source anisotropy, the plaque or insert materials of the plaques and also photon backscatter or fluorescence photons from the plaque backing. In the early 1990s, the beginning of the investigation of the effect of the plaque backing and material insert (such as Silastic) on dose distribution and the recommended dosimetry protocol for eye plaques was issued by the Task Group (TG) 129 report. This report includes the correction factors/formula for heterogeneous plaque materials (backing and insert material) [9–12]. Common isotopes used in ocular brachytherapy are ^{125}I , ^{103}Pd and ^{106}Ru . Iodine–125 is currently the most commonly used and well documented in the literature. Some few centers use palladium-103, observing that the low gamma emission of ^{103}Pd , 20 keV, presents less radiation exposure hazard to personnel [13]. But due to the low energy of the photons from ^{103}Pd , the effect of backscatter from plaque backing on dose distribution is expected to be significant. Many reports are available concerning the effect of the gold plaque backing on dose rate [14, 15]. They reported a dose enhancement near the seed due to the backscatter photons from the gold backing. Chiu-Tsao et al. [16], Thomson et al. [17] and de la Zerda et al. [12] reported that dose at small distances from the seed was reduced due to the presence of gold backing. In this work, the Monte Carlo technique is used to study dose rate distributions around the COMS gold eye plaques having diameters from 10 to 22 mm and fully loaded with a palladium seed. The seeds were distributed into Silastic insert inside the 10–22 mm diameter COMS eye plaques. As reported by the American Association of Physicists in Medicine (AAPM), TG-43U1 recommendations, before using each new source, the dosimetric characteristics of the source need to be determined to provide reliable data for use in treatment planning calculations [18]. As stated by TG-43U1 guidelines, we have calculated the dosimetric parameters of the IR06- ^{103}Pd source. As the internal components of the seed are free to move within the titanium capsule, their location can vary with seed orientations. In our Monte Carlo calculations, three geometric models of the seed (ideal, vertical and diagonal) were also developed. Since the tumour control rate for plaque brachytherapy is high, the most important issue is the side effects in healthy structures (points of interest) in the eye region. Doses at points of interest were calculated for selected plaque positions on the surface of an eye. Further Monte Carlo simulations have been employed to investigate the effect of plaque gold backing and Silastic inserts on dose distributions along the central axis of the eye plaque and at critical points in the eye region. To investigate the effect of the plaque backing and Silastic insert on dose distributions, four different configurations of plaque were simulated for the IR06-palladium seed model, namely:

1. Silastic insert with gold backing
2. Silastic insert with water replacing gold backing
3. Liquid water replacing Silastic, with gold
4. Liquid water replacing Silastic and gold (seeds alone in water)

Finally, dose along the plaque's central axis and at the critical points are compared with 125-I (6711 model) and $^{103}\text{-Pd}$ (Theragenics model 200) seeds loaded in COMS eye plaque [17].

2. Materials and methods

In this work, the Monte Carlo calculations have been performed to calculate the dose distribution around the eye plaque. The Monte Carlo method is a numerical technique using random numbers and probability to solve problems. It performs an effort to model nature through direct simulation for any possible results, by a probability distribution, for any cause that has inherent uncertainty. The name of this method comes from the casino name in Monaco, because of roulette, a simple random number generator. Clinical dose calculations are generally carried out with the patient treated as water equivalent and a dose of 85 Gy prescribed to the tumour apex. In the calculation the effects from the presence of the plaque backing, insert and intraocular media are considered [19]. In this work, the dose distributions were simulated using the MCNP5 Monte Carlo (MC) radiation transport code published by the Los Alamos National Laboratory, and the MCPLIB04 photon cross-section library is based on the ENDF/B-VI data [20]. The $^{103}\text{-Pd}$ photon spectrum used in these simulations was obtained from TG-43U1 table XIII [18]. To calculate absorbed dose and kerma, the particle fluence and cell-heating tallies, F4 and F6, have been used, respectively.

2.1 $^{103}\text{-Pd}$ source description

The source used in this study is the palladium-103 source model IR06- ^{103}Pd seed which is designed and fabricated in Agricultural, Medical and Industrial Research School (AMIRS). The production of $^{103}\text{-Pd}$ is carried out via the $^{103}\text{Rh}(p,n)^{103}\text{Pd}$ reaction which is well suited to low-energy cyclotrons. $^{103}\text{-Rh}$ target was irradiated via cyclotron (IBA-Cyclone30, Belgium) at the AMIRS. The solid targetry system in this cyclotron is made up of a pure copper backing on which the target materials are electrodeposited. The target that undergoes bombardments by the proton beam at the cyclotron production consists of three layers as follows: (I) rhodium layer, (II) copper layer and (III) copper layer without induced proton beam [21]. All irradiation of the electroplated Rh targets were performed at 200 μA beam current. The rhodium targets were prepared by the electrodeposition technique. Thus, the electrodeposition experiments were performed in acidic sulphate media using $\text{RhCl}_3 \cdot 3\text{H}_2\text{O}$, $\text{Rh}_2(\text{SO}_4)_3$. The radiochemical processing of the irradiation targets involved (a) dissolution, (b) radiochemical separation of $^{103}\text{-Pd}$ from the Rh target solution and (c) recovery of $^{103}\text{-Pd}$ as the final product from the organic phases [22]. After the chemical separation process, $^{103}\text{-Pd}$ radioactive material is absorbed uniformly in the resin Amberlite IR-93 resin (20–50 mesh) bead to encapsulate

inside the titanium capsule. The seed contains five resin beads, each in diameter of 0.6 mm with the compositions of (by weight percent) C, 90%; H, 8%; Pd, 1%; Cl, 0.7%; and N, 0.3%, with the density equal to 1.14 g/cm³. The resin beads are packed inside a titanium capsule of 4.7 mm length; 0.7 and 0.8 mm internal and external diameters, respectively; and 0.6 mm thick end caps and with an effective length of 3 mm. ¹⁰³Pd radioactive material is absorbed uniformly in the resin bead volume [23]. **Figure 1** shows a schematic diagram of the IR06-¹⁰³Pd seed. As the resin beads are free to move within the titanium capsule, their location can vary with seed orientations. Following the TG-43U1 recommendation for “good practice for Monte Carlo calculations” [18], mechanical mobility of the internal component of the seed has been considered in the simulations, and three geometric models (ideal, vertical and diagonal) of the seed were developed as shown in **Figure 1a–c**.

2.2 Seed Monte Carlo dosimetry

The IR06-¹⁰³Pd brachytherapy seed has been simulated in the center of a spherical water phantom in 15 cm radius with an array of 1 mm thick detector rings. Detectors were defined at distances of $r = 0.25, 0.5, 0.75, 1, 2, 3, 4, 5$ and 7 cm, away from the palladium-103 seed and at polar angles relative to the seed longitudinal axis from 0 to 90°. The rings were also bounded with two cones (10°) bisecting the phantom sphere corresponding to points in two-dimensional TG-43U1 dose formalism for ideal orientation and from 0 to 180° for vertical and diagonal orientations, with 10° increment. A cross section of the detector arrangement is shown in **Figure 2**.

To calculate the dosimetric parameters of the seed, TG43-U1 formalism has been used, which are briefly described by Sadeghi et al. [24].

According to TG43-U1 recommendation, the proposed formula for two-dimensional dose rate is

$$\dot{D}(r, \theta) = S_K \Lambda \frac{G(r, \theta)}{G(r_0, \theta_0)} g(r) F(r, \theta) \quad (1)$$

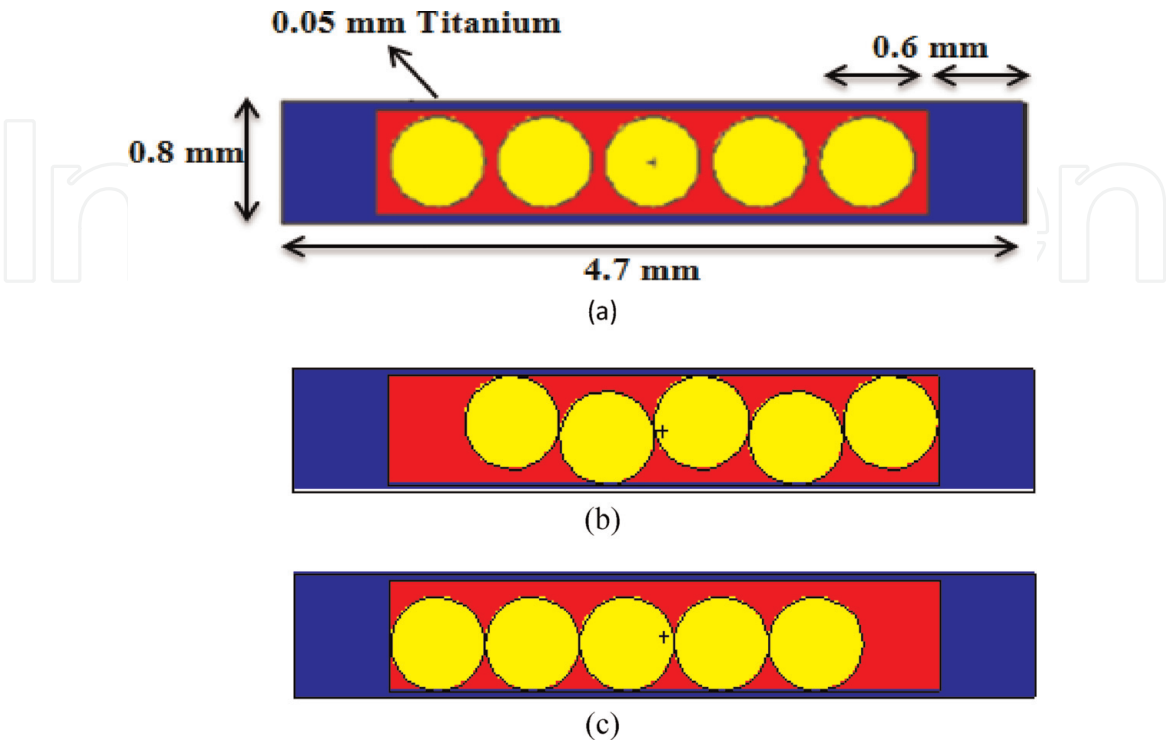


Figure 1. Schematic diagram of the IR06-¹⁰³Pd seed in (a) ideal, (b) diagonal and (c) vertical orientation.

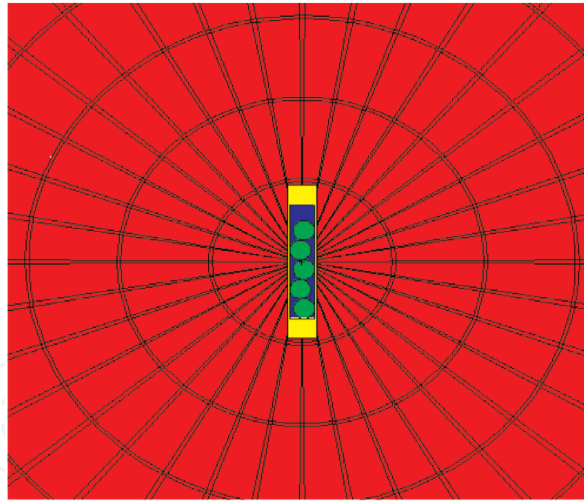


Figure 2.
 Cross section of the detector arrangement for Monte Carlo calculations.

where:

$\dot{D}(r, \theta)$ is the dose rate in the water at the distance r in cm from the source.

θ is the polar angle specifying the point of interest.

S_K is the air kerma strength and the unit is $U = \text{cGy cm}^2 \text{h}^{-1}$.

Λ is the dose rate constant with the unit of $\text{cGy h}^{-1} \text{U}^{-1}$.

$\frac{G(r, \theta)}{G(r_0, \theta_0)}$ is the geometry factor; $r_0 = 1 \text{ cm}$ and $\theta_0 = 90^\circ$ (reference position).

$g(r)$ and $F(r, \theta)$ are the radial dose function and the anisotropy function, respectively.

The dose rate constant, Λ , for the seed was calculated as the ratio of the dose to water at 1 cm from the seed along the transverse axis to the source's air kerma strength, S_K , at distance r from the source center. The air kerma strength was calculated using the following equation [18]:

$$S_K = \dot{K}_\delta(r) r^2 \quad (2)$$

As the energy of the photons from $^{103}\text{-Pd}$ are low, in the Monte Carlo calculations, all the generated electrons from the photon collisions are absorbed locally, so it was expected that dose is equal to kerma at all points of interest. The air kerma rate, $\dot{K}_\delta(r)$, of the seed was determined by calculating the dose in 1 mm thick air-filled rings in a vacuum. The rings were bounded by 86° and 94° conics and defined with a radial increment of 5–150 cm along the transverse axis of the source to find the SK that is independent to distance [14]. The dose distributions were calculated from the energy deposition averaged over a cell tally F6 in MeV/g/source photon. For the calculations, the titanium characteristic X-ray production was suppressed with $\delta = 5 \text{ keV}$ (δ is the energy cut-off) [25]. The radial dose function expresses the effect of tissue attenuation on photons emitted from seed and defines the dose fall-off along the seed transverse axis due to the attenuation and scattering of the photon. $g(r)$ was calculated by the following equation:

$$g_X(r) = \frac{\dot{D}(r, \theta_0)}{\dot{D}(r_0, \theta_0)} \frac{G_L(r_0, \theta_0)}{G_L(r, \theta_0)} \quad (3)$$

Dose variations, as the distribution of seed radioactivity, oblique filtration, and self-absorption in the encapsulating material, are defined by the 2D anisotropy function as follows:

$$F(r, \theta) = \frac{\dot{D}(r, \theta)}{\dot{D}(r, \theta_0)} \frac{G_L(r, \theta_0)}{G_L(r, \theta)} \quad (4)$$

The simulations were performed in water with 1×10^9 histories giving statistical uncertainties of 2.5 and 3.5% at 1 and 5 cm along the long axis and 0.05–0.1% at 1 and 5 cm on the transverse plane. The statistical uncertainty in the air was 1% with 7×10^7 histories. In this study, the Monte Carlo simulation was benchmarked with the brachytherapy seed model Theragenics 200 [18, 26].

2.3 Eye plaque simulation

To determine the dose rate around the eye plaque, eyeball and eye plaque, which are loaded with the seeds, are modelled in the center of $20 \times 20 \times 15 \text{ cm}^3$ water phantom. The seeds were distributed in the Silastic insert. The longitudinal axes of the seeds are perpendicular to the eye phantom central plane.

The total dose is calculated by the following equation [14]:

$$\dot{d}(x, y, z) = {}_{SP}\dot{d}(x, y, z) \left[{}_{source}S_K \left(\frac{SK}{A} \right)^{-1} K \right] .n \quad (5)$$

where $\dot{d}(x, y, z)$ is the dose rate at (x, y, z) position, S_k is the air kerma strength per history calculated by using Monte Carlo methods, A is the activity (mCi), K is the photons emitted per unit activity (photons mCi^{-1}) and n is the number of seeds which are loaded in the eye plaque. The COMS eye plaques which are used in this study are composed of two parts with diameters ranging from 10 to 22 mm in 2 mm increments:

- a. The gold backing, with the composition of (by weight) 77% gold, 14% silver, 8% 159 copper and 1% palladium and a density of 15.8 g/cm^3 [27]
- b. The Silastic insert as a seed carrier with the composition of (by weight) 6.3% hydrogen, 24.9% carbon, 28.9% oxygen, 39.9% silicon and 0.005% platinum and a density of 1.12 g/cm^3 [15]

The plaque assumed a standard eye diameter of 24.6 mm by considering lens and homogenized eye materials according to ICRU 46 [28]. The position of the points is followed by Thomson et al. [17] (Figure 3). The lens is modelled in the homogenized eye, and to obtain the dose rate, the plaque and eye ball are then modelled at the center of the spherical water phantom with 30 cm diameter. The plaque backing and Silastic insert effect on dose rate is obtained by replacing water with gold and Silastic insert. Central axis depth dose to water was determined using the F6 tally of MCNP for 0.05 mm radius and 0.01 mm thick cylindrical voxels from the outer sclera (−1 mm) to 11 mm inside the eye in 0.5 mm steps [2]. For the comparison doses to interest points (center of the eye, macula, optic disk, proximal sclera, tumour apex, lacrimal gland and retina opposite the apex) have been determined. The total dose is calculated following Melhus and Rivard [14] and Thomson et al. [17] verbatim: “The Monte Carlo simulations provide the dose in a voxel per history. The dose rate is calculated by dividing this number by the air kerma strength per history for the relevant seed type and multiplying by the number of seeds and the air kerma strength per seed. The air kerma strength per seed is chosen in order to obtain a prescription dose of 85Gy at the tumour apex (5 mm on the central axis) in 168 hours for $^{103}\text{-Pd}$. The total dose delivered during treatment is then

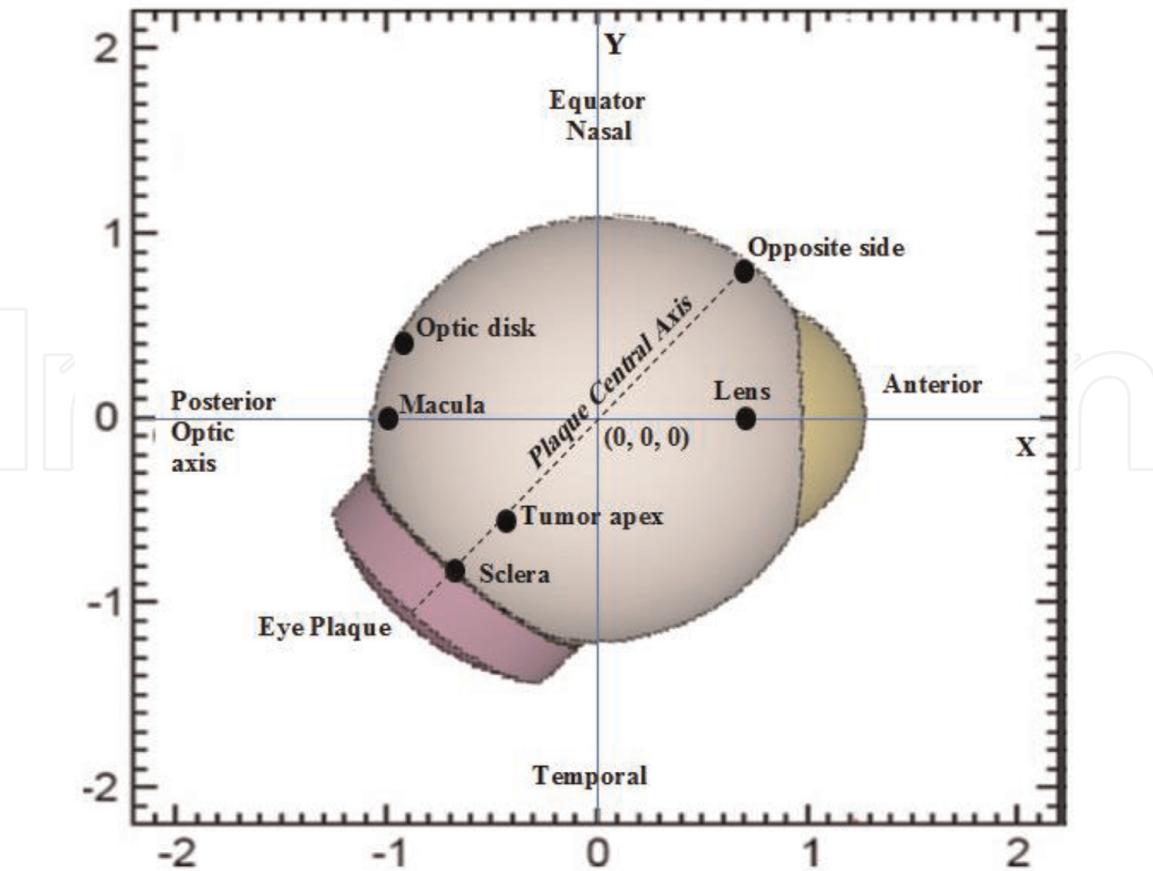


Figure 3.
Points of interest for eye plaque dosimetry, given in the center of eye reference frame (scale in centimeters) for a right eye [17]. In the figure a plaque midway between the posterior pole and equator temporal is shown. All points of interest are indicated (with the exception of the lacrimal gland, which does not lie in the plane shown).

determined by integrating over the treatment time, taking into account the exponential decay of the source”. Also, the photoelectric absorption, fluorescent emission and Rayleigh and Compton scattering, of characteristic K- and L-shell X-rays, are all simulated. For variance reduction, the electron and photon transport energy cut-off in all calculations was selected at 1 and 5 keV, respectively [29]. In the simulation 3.8×10^8 photon histories were simulated, and the statistical uncertainties at 5 and 11 mm (tumour apex) depth of central axis were obtained at 0.7 and 1.1%, respectively. Statistical uncertainties at the opposite side of the eye exceeded 4% which has the greatest uncertainty among the points on interest.

3. Results and discussions

3.1 Seed dosimetry benchmarking

In this work, the Monte Carlo simulation was benchmarked with the Theragenics model 200 source. The comparison between the calculated value of Λ for the model 200 in this study, $0.685 \text{ cGy h}^{-1} \text{ U}^{-1}$, and the previously published data for the seed [18], $0.686 \text{ cGy h}^{-1} \text{ U}^{-1}$ ($\sim 0.1\%$ difference), shows the accuracy of our simulation method. The result has been presented in **Table 1**. Based on the calculations, the dose rate constant for the IR06- ^{103}Pd source in ideal orientation is estimated to be $0.692 \pm 0.020 \text{ cGy} \cdot \text{h}^{-1} \cdot \text{U}^{-1}$ which is comparable with the other two commercial sources. Calculated S_K per contained activity for model 200 in this work was 0.722 U mCi^{-1} . The result was compared to 0.721 U mCi^{-1} for Williamson’s WAFAC simulation, [26] and Melhus et al. [14] calculations. The values of Λ in three seed orientations ranged from 0.689 to $0.697 \text{ cGy h}^{-1} \text{ U}^{-1}$, with a 0.34%

Source type	Method	Medium	Λ (cGy h ⁻¹ U ⁻¹)
IR06- ¹⁰³ Pd	Monte Carlo simulation (ideal) ^a	Liquid water	0.692 ± 0.021
	Monte Carlo simulation (diagonal) ^a	Liquid water	0.697 ± 0.021
	Monte Carlo simulation (vertical) ^a	Liquid water	0.689 ± 0.021
MED3633	TLD dosimetry ^b	Solid water	0.688 ± 0.05
	Monte Carlo simulation ^c	Liquid water	0.677 ± 0.02
Theragenics model 200	TLD dosimetry ^d	Solid water	0.650 ± 0.08
	Monte Carlo simulation ^e	Liquid water	0.686 ± 0.03
	Monte Carlo simulation ^a	Liquid water	0.685 ± 0.02
Best model 2335	TLD dosimetry ^f	Solid water	0.69 ± 0.08
	Monte Carlo simulation ^f	Liquid water	0.67 ± 0.02

^aPresent work.
^bRef. [33].
^cRef. [34].
^dRef. [32].
^eRef. [26].
^fRef. [27].

Table 1. Monte Carlo calculated dose rate constant, Λ , of the IR06-¹⁰³Pd and model 200 seeds in comparison with the measured and calculated values of model MED3633, model 200 and model 2335 seeds.

uncertainty. According to TG-43U1, a standard uncertainty of 3% is acceptable for Monte Carlo studies. The dose rate constant can be calculated by normalizing to the S_K of the vertical orientation and the source geometry during the NIST calibration. The values, in this case, are 0.680 ± 0.020 cGy h⁻¹ U⁻¹, ~1.7% lower than the value in the ideal orientation. This result obtained in this study is comparable with Λ values obtained for other ¹⁰³-Pd sources which are presented in TG-43U1 report. **Table 1** shows the calculated dose rate constant for the IR06-¹⁰³Pd seed and the measured and calculated values of Λ , for NASI model MED3633, Theragenics model 200 and Best model sources.

The calculated line radial dose function $g_L(r)$, of the IR06-¹⁰³Pd for ideal orientation, was fit to a fifth-order polynomial function yielding the following relationship:

$$g_L(r) = a_0 + a_1r + a_2r^2 + a_3r^3 + a_4r^4 + a_5r^5 \tag{6}$$

where:
 $a_0 = 1.785$, $a_1 = -1.064$, $a_2 = 3.385 \times 10^{-1}$, $a_3 = -7.062 \times 10^{-2}$, $a_4 = 8.469 \times 10^{-3}$ and $a_5 = -4.173 \times 10^{-4}$ define $R^2 = 9.999 \times 10^{-1}$.

Figure 4 presents the radial dose function, $g(r)$, for IR06-¹⁰³Pd seed and three other commercial sources. **Table 2** shows the differences between the results of this study and AAPM TG-43U1 reference data for model 200. As the differences are <3%, the agreement between these data sets is acceptable. The radial dose function values for two other geometric models, vertical and diagonal, were also calculated, and the disagreement between them varied from <2%. The anisotropy function, $F(r, \theta)$, of the IR06-¹⁰³Pd seed was calculated in the phantom of water, at radial distances of $r = 0.25, 0.5, 0.75, 1, 1.5, 2, 3, 4, 5$ and 7 cm relative to the seed center and polar angle, θ , ranging from 0 to 180° for vertical and diagonal orientations and $0-90^\circ$ for ideal orientation, in 10° increment with respect to the seed long axis. The results are shown in **Table 3**.

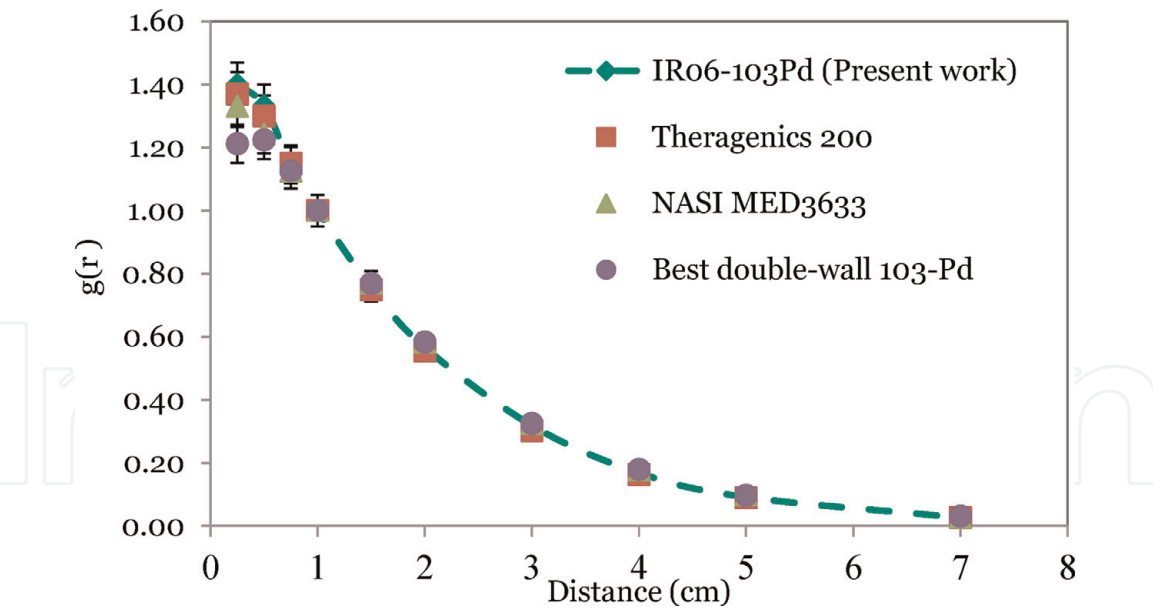


Figure 4. Comparison of the calculated radial dose function of IR06- ^{103}Pd seeds in water versus other available sources [18, 30].

r (cm)	$g_L(r)$		
	Theragenics 200		IR06- ^{103}Pd
	Ref. [26]	Present work	
0.5	1.300	1.330	1.333
0.75	1.150	1.170	1.144
1	1.000	1.000	1.000
1.5	0.749	0.755	0.756
2	0.555	0.567	0.566
3	0.302	0.305	0.318
4	0.163	0.168	0.168
5	0.089	0.091	0.091
7	0.026	0.027	0.026

Table 2. Monte Carlo calculations for radial dose function, $g_L(r)$, for IR06- ^{103}Pd and model 200 seeds compared to reference Monte Carlo data.

Figure 5 shows a comparison between the calculated anisotropy function of the IR06- ^{103}Pd seeds at a distance of 2 cm from the source center in water with the other published data (in ideal orientation). The values of the anisotropy function for the new $^{103}\text{-Pd}$ sources agreed with those for the model MED3633, Theragenics model 200 and Best® double-wall $^{103}\text{-Pd}$ sources [18, 26, 30] are found in 4% in angles $>20^\circ$. Due to the thick end caps of the IR06- ^{103}Pd source, the differences in smaller angles can be as large as up to 17%.

3.2 Plaque Monte Carlo simulations

Table 4 shows the calculated central depth dose distribution for COMS eye plaques loaded with IR06- ^{103}Pd seeds in the Silastic insert.

The depth dose distribution has been calculated in 0.5 mm steps between the outer sclera (−1 mm) to 3 mm and in 1 mm steps from 4 to 10 mm. The dose distribution is also calculated in water medium to obtain the effect of the Silastic insert and the plaque backing on central axis dose distribution. In this study, the

a. 2-D anisotropy function, F(r,θ), in ideal seed orientation										
r (cm)	Θ=									
	0°	10°	20°	30°	40°	50°	60°	70°	80°	90°
0.25	0.053	0.074	0.616	0.854	0.924	0.959	0.979	0.992	0.998	1.000
0.5	0.132	0.165	0.472	0.701	0.845	0.927	0.964	0.985	0.996	1.000
0.75	0.169	0.211	0.480	0.686	0.823	0.912	0.960	0.985	0.997	1.000
1	0.190	0.242	0.491	0.686	0.816	0.903	0.956	0.982	0.996	1.000
1.5	0.229	0.281	0.512	0.692	0.813	0.899	0.952	0.982	0.995	1.000
2	0.265	0.309	0.526	0.696	0.814	0.896	0.950	0.982	0.996	1.000
3	0.294	0.345	0.545	0.705	0.815	0.897	0.949	0.981	0.997	1.000
4	0.319	0.369	0.558	0.709	0.818	0.895	0.948	0.979	0.995	1.000
5	0.337	0.392	0.568	0.715	0.820	0.900	0.948	0.981	0.995	1.000
7	0.405	0.428	0.601	0.730	0.831	0.900	0.948	0.982	1.004	1.000
b. 2-D anisotropy function, F(r,θ), in vertical seed orientation										
r (cm)	Θ=									
	0°	10°	20°	30°	40°	50°	60°	70°	80°	90°
0.25	1.155	0.471	0.526	0.591	0.568	0.504	0.426	0.351	0.308	1.000
0.5	0.958	0.436	0.485	0.597	0.650	0.672	0.682	0.695	0.720	1.000
0.75	0.931	0.453	0.508	0.631	0.702	0.743	0.775	0.806	0.840	1.000
1	0.907	0.471	0.531	0.656	0.733	0.784	0.823	0.856	0.895	1.000
1.5	0.900	0.497	0.560	0.685	0.767	0.824	0.868	0.905	0.945	1.000
2	0.880	0.514	0.579	0.704	0.786	0.845	0.888	0.928	0.967	1.000
3	0.859	0.541	0.606	0.724	0.810	0.867	0.912	0.952	0.992	1.000
4	0.851	0.557	0.623	0.737	0.817	0.875	0.924	0.961	1.004	1.000
5	0.810	0.577	0.637	0.747	0.826	0.883	0.927	0.968	1.009	1.000
7	0.889	0.610	0.668	0.769	0.846	0.901	0.946	0.977	1.024	1.000
r (cm)	100°	110°	120°	130°	140°	150°	160°	170°	180°	
0.25	0.945	0.682	0.877	0.942	0.975	0.993	1.003	1.005	1.002	
0.5	0.918	0.652	0.741	0.855	0.933	0.974	0.994	1.003	1.002	
0.75	0.887	0.661	0.739	0.837	0.916	0.964	0.989	1.000	1.001	
1	0.874	0.673	0.743	0.835	0.908	0.960	0.988	1.000	1.001	
1.5	0.856	0.685	0.753	0.837	0.906	0.956	0.985	0.999	1.001	
2	0.851	0.696	0.758	0.840	0.905	0.954	0.984	0.998	1.001	
3	0.845	0.712	0.768	0.845	0.907	0.954	0.984	0.998	1.001	
4	0.842	0.722	0.778	0.848	0.907	0.953	0.983	0.997	1.000	
5	0.839	0.733	0.785	0.853	0.909	0.953	0.983	0.996	1.000	
7	0.852	0.757	0.805	0.869	0.919	0.963	0.988	1.003	1.004	

c. 2-D anisotropy function, F(r,θ), in diagonal seed orientation										
r (cm)	Θ=									
	0°	10°	20°	30°	40°	50°	60°	70°	80°	90°
0.25	1.155	0.471	0.525	0.591	0.567	0.502	0.424	0.352	0.310	1.000
0.5	0.969	0.438	0.485	0.597	0.651	0.673	0.682	0.696	0.723	1.000
0.75	0.941	0.453	0.508	0.631	0.701	0.744	0.775	0.805	0.842	1.000
1	0.918	0.471	0.530	0.657	0.734	0.783	0.822	0.857	0.897	1.000
1.5	0.907	0.497	0.560	0.686	0.767	0.824	0.866	0.906	0.947	1.000
2	0.881	0.515	0.579	0.704	0.786	0.845	0.889	0.930	0.972	1.000
3	0.857	0.540	0.607	0.724	0.806	0.865	0.910	0.953	0.995	1.000
4	0.852	0.556	0.623	0.738	0.817	0.873	0.921	0.962	1.003	1.000
5	0.810	0.577	0.637	0.746	0.825	0.883	0.928	0.969	1.012	1.000
7	0.888	0.610	0.669	0.769	0.846	0.902	0.946	0.979	1.027	1.000
r (cm)	100°	110°	120°	130°	140°	150°	160°	170°	180°	
0.25	0.945	0.684	0.879	0.943	0.974	0.993	1.002	1.003	1.004	
0.5	0.921	0.652	0.741	0.856	0.935	0.975	0.994	1.002	1.003	
0.75	0.889	0.663	0.739	0.837	0.915	0.964	0.989	1.001	1.002	
1	0.876	0.673	0.744	0.836	0.910	0.961	0.989	1.000	1.002	
1.5	0.860	0.686	0.752	0.837	0.905	0.956	0.985	0.999	1.001	
2	0.852	0.697	0.758	0.841	0.905	0.955	0.984	0.999	1.001	
3	0.847	0.713	0.769	0.845	0.906	0.954	0.984	0.998	1.002	
4	0.843	0.723	0.778	0.848	0.907	0.954	0.983	0.997	1.001	
5	0.842	0.733	0.785	0.853	0.908	0.953	0.983	0.996	1.000	
7	0.856	0.759	0.806	0.868	0.919	0.963	0.988	1.003	1.005	

Table 3.
2-D anisotropy functions for the IRO6-¹⁰³Pd seed calculated by Monte Carlo method for the (a) ideal orientation, (b) vertical orientation and (c) diagonal orientation.

required air kerma strength per seed (S_K) is calculated to deliver prescription dose (85 Gy) to the apex of the tumour (5 mm depth) for 168 hours of implant. In addition, to investigate the effect of different materials constituting the COMS plaque on dose distributions near the plaque, the ratio of dose in three media (discussed above) relative to dose in water medium is shown in **Figure 6**.

3.3 Effect of the gold backing

The effect of 20 mm gold plaque backing on dose distribution along the central axis is shown in **Figure 7**, which provides central axis depth dose curve for full loaded IRO6-¹⁰³Pd, Theragenics 200 and model 2335 seeds with water replacing the Silastic. This figure demonstrates dose is increased near the plaque; now this well-known effect is due to L-shell fluorescence photons emitted by atoms in the plaque backing [27]. Emission photons from palladium seeds with an average energy of about 21 keV excite the L-shell in gold and silver [31] which are the composition of the plaque backing. The excitation of these shells results in the emission of fluorescence photons, so this event explains why dose increases near the plaque. About

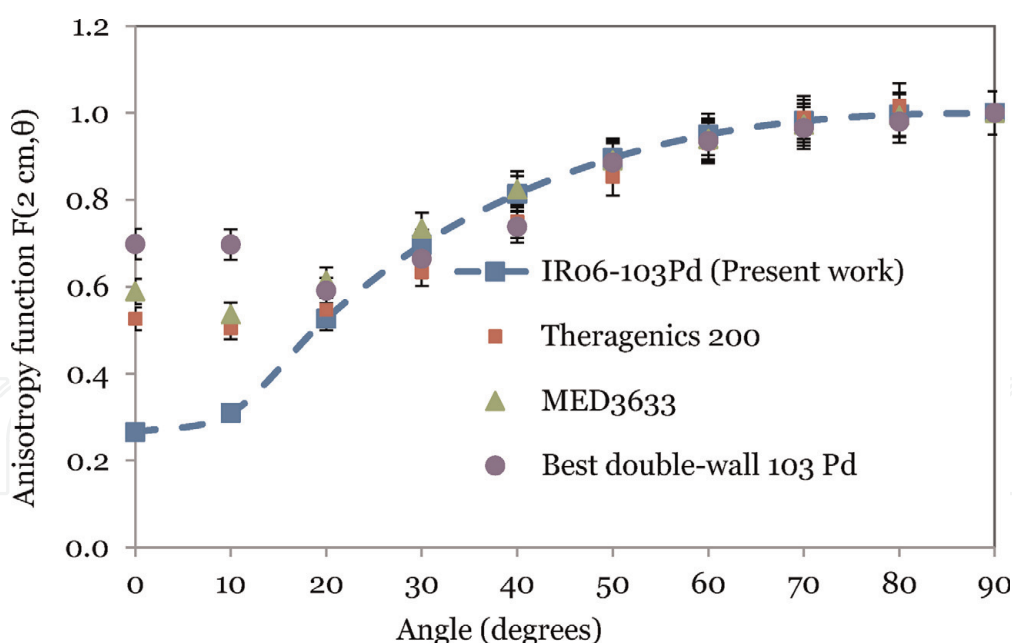


Figure 5.

Comparison of the calculated anisotropy function of the IR06- ^{103}Pd seed versus other available sources at 2 cm [18, 30].

0.7% dose enhancement is observed near the plaque which is loaded with IR06- ^{103}Pd seeds, but as the fluorescence photons are absorbed (mean free path is about 2 mm), after a few millimeters, the dose decreases in the order of 6.5%. In Thomson et al. [17] work, a dose decrease of about 6–6.3% at the opposite side of the eye for ^{103}Pd (Theragenics model 200) seed in gold backing (no Silastic) was reported. Chiu-Tsao et al. reported a dose decrease of about 10% for ^{125}I (model 6711) seed with 20 mm gold plaque (no Silastic) at 7.6 mm. Since the emitted photons from the ^{125}I seed have higher energy than those emitted by ^{103}Pd seed, more fluorescence photons are observed when ^{125}I source is used. Due to the emission of fluorescence photons from the plaque backing for all seed and backing models without any polymer insert, there is a small dose enhancement near the plaque. The spectrum of fluorescence photons depends on the energy of photons emitted by the seed and its active length and also depends on the composition of plaque backing.

3.4 Effect of silastic insert

The central axis doses for the IR06- ^{103}Pd seeds in Silastic insert with plaque backing are shown in **Figure 8** relative to the doses for the same seeds in the water medium. Silastic with an effective atomic number of ~ 10.7 has a greater attenuating effect than water with an effective atomic number of $Z_{\text{eff}} (\sim 7.4)$ [17]. The average variation in dose distribution due to Silastic insert relative to water is about 17%. Thomson et al. [27] reported 17% dose reduction for Theragenics model 200 ^{103}Pd seed at a distance of 1 cm in COMS plaque due to the presence of Silastic insert. Chiu-Tsao et al. [16] calculated a 10% dose reduction at 1 cm for Silastic insert only, in 20 mm COMS eye plaque for ^{125}I , and 16% for ^{103}Pd (without gold backing) relative to water along the central axis; according to their study also, they presented that the effect of gold + Silastic combination is comparable with the effect of Silastic insert only. The reduction of dose for ^{125}I source in Silastic insert is more than ^{103}Pd source due to its higher energy of emitted photons. The dose reduction for the gold + Silastic combination relative to water medium as shown in **Figures 6 and 8** is

Central axis depth (mm)	a. Gold backing + Silastic						
	IR06- ¹⁰³ Pd seeds						
	COMS eye plaque diameter (mm)						
	10	12	14	16	18	20	22
−1	582.3	462.1	411.1	325.7	309.1	297.4	300.3
−0.5	474.1	401.5	375.2	305.5	296.3	232.3	298.5
0	380.7	325.8	302.1	271.5	264.3	212.8	254.7
0.5	312.5	300.0	267.4	250.7	220.2	202.8	222.8
1	302.7	248.6	220.2	243.9	189.2	176.4	196.8
1.5	254.8	220.1	215.3	214.4	180.5	167.8	178.7
2	198.4	190.5	170.0	188.9	168.7	159.8	168.2
2.5	180.8	183.7	162.5	164.3	152.4	140.6	154.6
3	148.9	150.3	130.8	148.2	132.8	122.7	155.2
4	120.3	105.1	110.2	120.4	108.7	100.2	104.5
5 (Apex)	85.0	85.0	85.0	85.0	85.0	85.0	85.0
6	63.7	64.1	72.5	80.0	78.2	69.5	72.4
7	50.0	50.0	52.4	69.2	60.5	58.4	60.1
8	32.4	35.2	35.3	55.4	48.9	55.1	51.2
9	28.4	29.8	34.8	40.5	41.5	38	40.5
10	22.5	24.6	28.9	28.8	33.1	35.5	34.4
$S_K(U)$	10.88	7.11	5.1	5.23	3.52	3.33	3.61
Central axis depth (mm)	b. Gold backing + Silastic						
	¹⁰³ Pd model 200 seeds [14]						
	COMS eye plaque diameter (mm)						
	10	12	14	16	18	20	22
−1	640.1	479.9	406.9	279.0	306.2	272.0	310.3
−0.5	547.0	423.8	368.7	277.7	281.2	252.7	278.1
0	452.4	366.5	322.4	259.1	250.6	227.6	242.1
0.5	376.3	313.1	278.8	234.2	221.7	204.6	213.0
1	313.8	268.0	241.9	210.4	198.5	183.8	187.9
1.5	260.6	230.2	211.9	189.1	177.8	166.5	166.2
2	218.2	199.1	185.4	169.0	160.7	151.3	150.4
2.5	183.8	171.0	162.0	151.3	143.9	137.2	136.7
3	155.5	147.1	142.5	134.1	129.9	124.9	123.6
4	113.4	111.0	109.6	107.2	105.5	102.9	102.4
5 (Apex)	85.0	85.0	85.0	85.0	85.0	85.0	85.0
6	64.7	65.8	67.2	68.1	69.8	70.2	70.8
7	49.7	51.8	53.4	54.3	56.8	57.8	58.6
8	39.3	41.3	42.7	44.1	46.6	48.3	48.7
9	31.2	32.7	34.4	36.1	38.1	40.0	40.9
10	25.2	26.1	28.1	29.4	31.9	33.1	34.6
$S_K(U)$	11.057	7.299	4.809	5.062	3.405	3.139	3.738

Central axis depth (mm)	c. Gold backing + Silastic/water medium						
	IR06- ¹⁰³ Pd seeds						
	COMS eye plaque diameter (mm)						
	10	12	14	16	18	20	22
−1	0.74	0.72	0.71	0.65	0.68	0.66	0.71
−0.5	0.75	0.75	0.73	0.72	0.73	0.72	0.73
0	0.76	0.76	0.76	0.73	0.76	0.73	0.76
0.5	0.78	0.78	0.78	0.77	0.77	0.76	0.77
1	0.80	0.80	0.79	0.79	0.79	0.79	0.78
1.5	0.81	0.81	0.81	0.81	0.8	0.79	0.78
2	0.81	0.81	0.81	0.81	0.81	0.80	0.78
2.5	0.81	0.81	0.81	0.81	0.81	0.80	0.79
3	0.81	0.81	0.81	0.81	0.82	0.80	0.81
4	0.81	0.81	0.81	0.81	0.82	0.80	0.81
5 (Apex)	0.81	0.81	0.81	0.81	0.82	0.81	0.81
6	0.80	0.80	0.81	0.8	0.82	0.81	0.81
7	0.80	0.80	0.81	0.8	0.82	0.81	0.81
8	0.80	0.80	0.81	0.8	0.82	0.81	0.81
9	0.80	0.80	0.81	0.81	0.81	0.83	0.80
10	0.80	0.80	0.81	0.81	0.81	0.83	0.80
$S_K(U)$	8.87	6.12	4	4.13	2.75	2.45	3.07

Table 4. Central axis dose distributions: (a) in 10–22 mm diameter COMS eye plaques (gold backing + Silastic insert) loaded with IR06-¹⁰³Pd seeds, (b) gold backing + Silastic insert loaded with ¹⁰³Pd model 200 seeds [14] and (c) the ratio of the central axis dose of the 10–22 mm COMS plaque (gold backing + silastic) to the central axis dose in water medium loaded with IR06-¹⁰³Pd seeds.

about 19% at 1 cm and 17% and at 0.5 cm, and the average dose reduction due to the presence of gold backing + Silastic insert along the COMS central axis loaded with the new palladium seeds is about 18%. Thomson et al. have obtained a reduction of the dose relative to water of 20% for ¹⁰³-Pd seed at 1 cm in the COMS plaque central axis; the main reduction is due to the Silastic insert. The comparison shows that the dose reduction with IR06-¹⁰³Pd seeds is lower along the central axis of the plaque with the exception of sclera than the other two palladium seed models, Theragenics 200 and model 2335 loaded in COMS plaque.

3.5 Dose comparison at points of interest

To determine the effect of plaque backing and Silastic insert on dose rate at points of interest, more Monte Carlo simulations were employed by replacing the plaque backing and Silastic inserts with water. **Table 5** presents the dose (in Gy) at points of interest for different plaque materials of 20 and 16 mm COMS plaque fully loaded with IR06-¹⁰³Pd seeds. To obtain the dose at the points of interest in a water

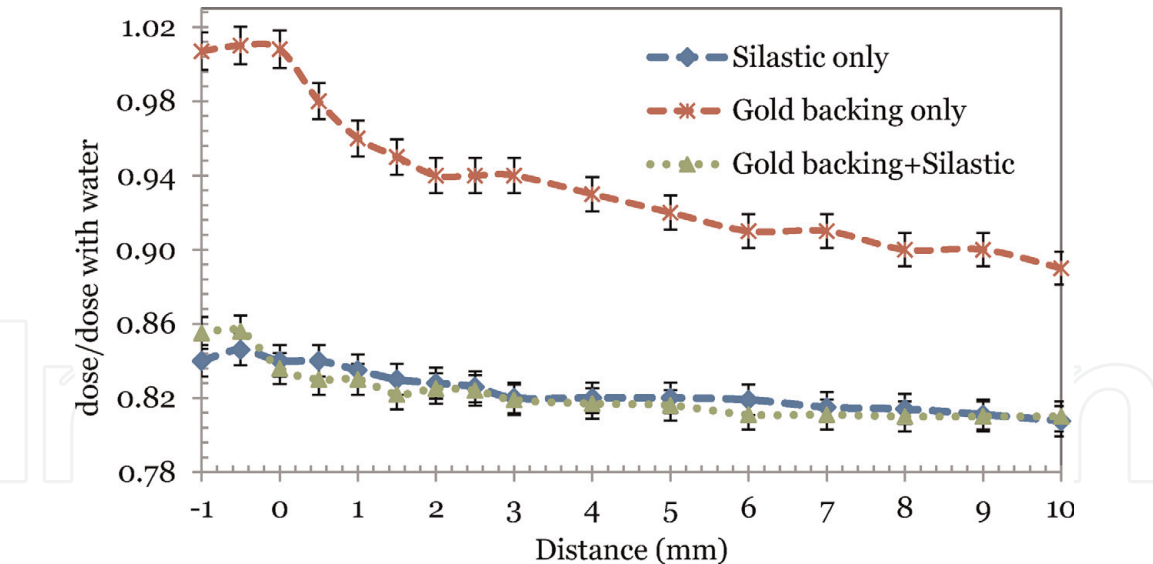


Figure 6.
Ratio of the doses along the plaque's central axis for 20 mm COMS plaque fully loaded with $\text{IR06-}^{103}\text{Pd}$ to the doses in water medium.

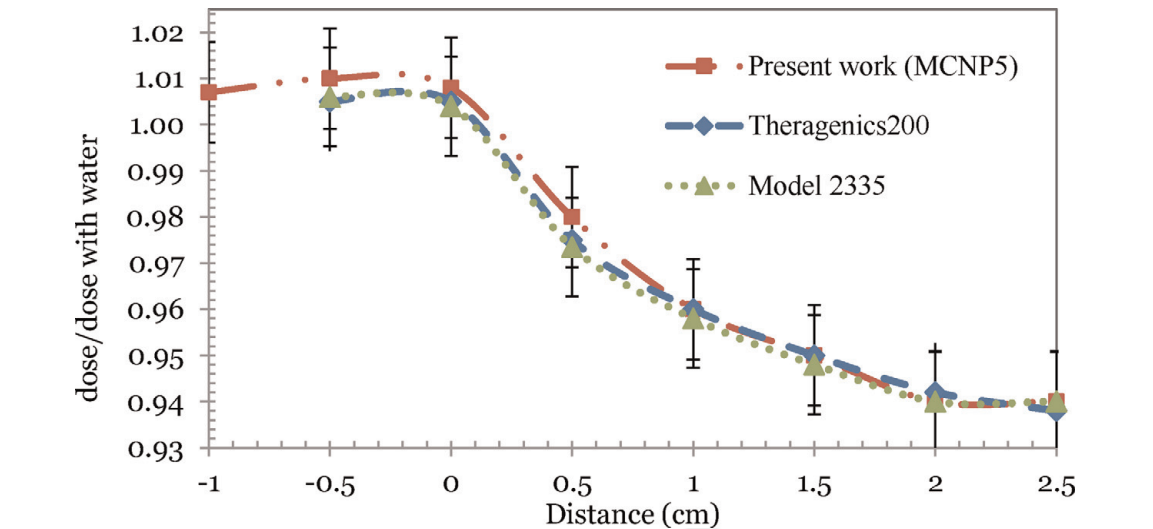


Figure 7.
Ratio of the doses along the plaque's central axis for 20 mm COMS plaque (no Silastic insert) loaded with $\text{IR06-}^{103}\text{Pd}$, model 200 and model 2335 seeds to the doses in water medium.

medium, the air kerma strength for each seed, (SK), is required to deliver 85 Gy to the tumour apex in 168 hours. All of the results have been renormalized to deliver the same dose (85 Gy) to the apex of the tumour. The results are compared with the dose at the same points when COMS plaque is loaded with Theragenics model 200 and 6711-125I seeds. According to **Table 5**, dose decreases at the optic disk by $\sim 40\%$ when moving a plaque from nasal to temporal equatorial centers. This is due to the fact that the optic disk is not centered on the eye anterior-posterior (AP) axis and is nearer the nasal plaque. For the plaque position between the posterior pole and equator temporal to the eyeball, the decrease in dose is due to the gold backing, and Silastic insert related to water medium is about 14% for $\text{IR06-}^{103}\text{Pd}$ seed and 21% for the model 200 at the opposite side of the eye [17]. When compared to identical plaques loaded with model 6711 125I sources, the doses at points of interest are consistently lower in plaque loaded with any of the $^{103}\text{-Pd}$ models in this study.

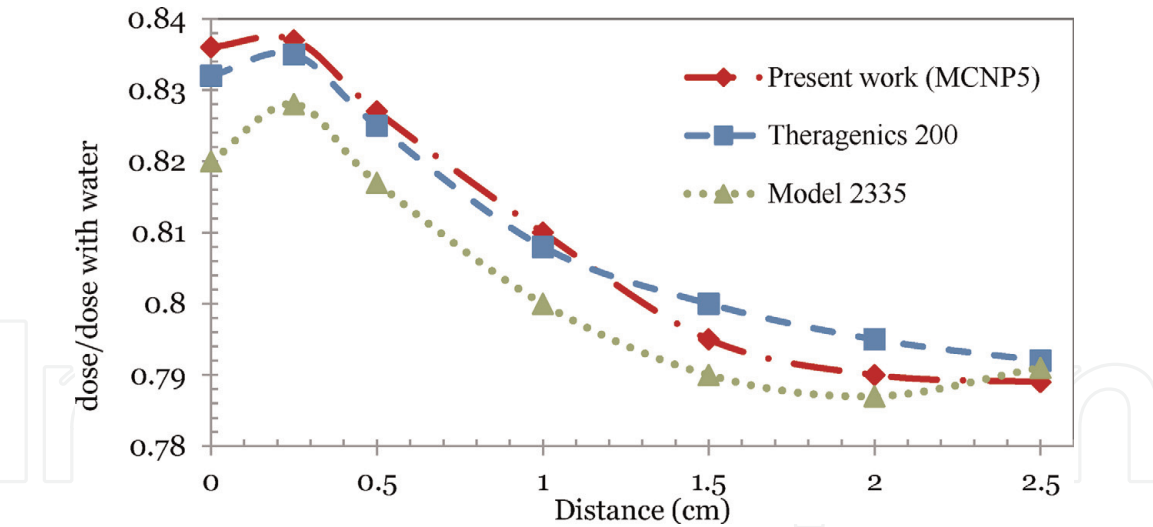


Figure 8. Ratio of the doses along the plaque’s central axis for 20 mm COMS plaque (gold backing + Silastic insert) fully loaded with IR06-¹⁰³Pd, model 200 and model 2335 seeds [17] to the doses in water medium.

Points of interest	a. 20 mm COMS			
	IR06- ¹⁰³ Pd ^a			
	Water medium	Silastic insert only	Gold backing only	Gold backing + Silastic
Centre of eye	29.08	34.31	30.82	34.37
Macula (equator and p.p)	15.57	17.22	16.55	18.29
Optic disk (temporal)	7.52	8.81	7.98	8.85
Optic disk (nasal)	18.29	21.47	19.42	21.44
Centre of lens (equator and p.p)	16.21	18.98	17.23	19.00
Sclera	351.81	367.38	374.68	383.73
Apex	85.00	85.00	85.00	85.00
Lacrimal gland (nasal)	4.82	5.59	5.12	5.62
Opposite side	3.39	3.94	3.59	3.95

	b. 16 mm COMS				
	Water medium		Gold backing + Silastic		
	IR06- ¹⁰³ Pd ^a	Theragenics 200 ^b	IR06- ¹⁰³ Pd ^a	Theragenics 200 ^b	6711- ¹²⁵ I ^c
Centre of eye	22.52	22.75	17.8	18.3	23.79
Macula (equator and p.p)	10.61	11.43	9.8	8.089	12.82
Optic disk (temporal)	6.32	7.193	5.12	5.35	8.98
Optic disk (nasal)	19.63	21.65	13.67	14.13	21.02
Centre of lens (equator and p.p)	15.63	16.34	11.83	12.5	17.58
Sclera	297.41	287.92	261.4	211	222.9
Apex	85.00	85.00	68.23	68.7	74.43
Lacrimal gland (nasal)	3.72	—	2.75	3.03	—
Opposite side	3.63	3.77	2.22	2.94	5.55

^aPresent work.
^bRef. [17].
^cRef. [27].

Table 5. Doses in grey at points of interest for (a) 20 mm (b) 16 mm COMS eye plaque loaded with IR06-¹⁰³Pd seeds compared with the doses at the same points for model 200 (¹⁰³Pd) and model 6711 (¹²⁵I), in 16 mm COMS eye plaque. Eye plaque centered in the midway of equator and posterior pole (equator and p.p) and centered on equator temporal and nasal.

4. Conclusion

In this study, the dosimetry of a new design brachytherapy seed IR06- ^{103}Pd was determined by Monte Carlo using MCNP (version 5). Simulations were considered in three seed orientations with the result that there are no significant statistical differences among the orientations (i.e., ideal, vertical and diagonal). The dosimetric parameters of the new seed are presented in TG-43U1 format. These parameters are in acceptable agreement with those of other commercially available seed models. Thus, the IR06- ^{103}Pd seed is dosimetrically suitable for use in routine brachytherapy where the other similar seeds are employed. Also in this study, the dosimetry of IR06- ^{103}Pd seed was evaluated in COMS eye plaques and compared to results for commercially available $^{103}\text{-Pd}$ and 125I seeds in the same plaque geometries.

The COMS Silastic insert has a significant effect in reducing dose along the plaque central axis. The presence of gold backing enhances the dose near the plaque gold surfaces. This effect is due to secondary fluorescence photons arising from the backing material. Due to the energy of these emissions, the effect is significantly attenuated at a distance >2 mm. The dose decrease depends on the composition of the plaque backing material and therefore on the emitted photon spectrum of the seeds and the fluorescence of the backing material.

The combination of gold backing with the Silastic insert decreases the dose relative to water by 19% at 1 cm along the plaque central axis.

This study shows that this 19% effect is lower than for either model 200 or 2335 $^{103}\text{-Pd}$ seeds. Doses to interest points including the macula, optic disk, lens, sclera and lacrimal gland have been determined; and also the effects of plaque backing material and Silastic insert have also been studied at these points. The study affirms that dose and dose rate at these points of interest in COMS plaques are routinely lower when using $^{103}\text{-Pd}$ rather than 125-I seeds. The dose to the proximal sclera, underlying the plaque, is greater using $^{103}\text{-Pd}$ seeds due to lessened penetration than 125-I seeds.

Author details


Pooneh Saidi^{1*} and Mahdi Sadeghi²

¹ Parsikan Iran Engineering and Management Consultants, Tehran, Iran

² Medical Physics Department, School of Medicine, Iran University of Medical Sciences, Tehran, Iran

*Address all correspondence to: poonehsaidi@gmail.com

IntechOpen

© 2019 The Author(s). Licensee IntechOpen. This chapter is distributed under the terms of the Creative Commons Attribution License (<http://creativecommons.org/licenses/by/3.0>), which permits unrestricted use, distribution, and reproduction in any medium, provided the original work is properly cited. 

References

- [1] Maheshwari A, Finger PT. Cancers of the eye. *Cancer and Metastasis Reviews*. 2018;**37**(4):677-690. DOI: 10.1007/s10555-018-9762-9
- [2] Saidi P, Sadeghi M, Shirazi A, Tenreiro C. ROPES eye plaque brachytherapy dosimetry for two models of ^{103}Pd seeds. *Australasian Physical & Engineering Sciences in Medicine*. 2011;**34**:223-231. DOI: 10.1007/s13246-011-0069-1
- [3] Rivard MJ, Melhus CS, Sioshansi S, Morr J. The impact of prescription depth, dose rate, plaque size, and source loading on the central axis using ^{103}Pd , ^{125}I , and ^{131}Cs . *Brachytherapy*. 2008;**7**:327-335. DOI: 10.1016/j.brachy.2008.05.002
- [4] Robertson DM. Changing concepts in the management of choroidal melanoma. *American Journal of Ophthalmology*. 2003;**136**:161-170. DOI: 10.1016/S0002-9394(03)00265-4
- [5] Finger PT. Radiation therapy for choroidal melanoma. *Survey of Ophthalmology*. 1997;**42**:215-232
- [6] Nag S, Quivey J, Earle J, Followill D, Fontanesi J, Finger PT. The American brachytherapy society recommendations for brachytherapy of uveal melanomas. *International Journal of Radiation Oncology, Biology, Physics*. 2003;**56**:544-555. DOI: 10.1016/S0360-3016(03)00006-3
- [7] Char DH, Kroll S, Quivey JM, Castro J. Long term visual outcome of radiated uveal melanomas in eyes eligible for randomisation to enucleation versus brachytherapy. *The British Journal of Ophthalmology*. 1996;**80**(2):117-124. DOI: 10.1136/bjo.80.2.117.
- [8] Melia BM, Abramson DH, Albert DM, Boldt HC, Earle JD, Hanson WF, et al. Collaborative ocular melanoma study (COMS) randomized trial of ^{125}I brachytherapy for medium choroidal melanoma, I. Visual acuity after 3 years: COMS report no. 16. *Ophthalmology*. 2001;**108**:348-366. DOI: 10.1016/S0161-6420(00)00526-1
- [9] Collaborative Ocular Melanoma Study Group. COMS Manual of Procedures PB95-179693. Ch 12. Springfield, VA: National Technical Information Service; 1995
- [10] Mourtada F, Chiu-Tsao S, Astrahan M, Finger P, Followill D, Meigooni A, et al. WE-D-BRB-01: Eye plaque dosimetry: Report of the AAPM therapy physics committee task group no. 129. *Medical Physics*. 2009;**36**(6):2771-2772. DOI: 10.1118/1.3182515
- [11] Morrison H, Menon G, Larocque MP, van Veelen B, Niatetski Y, Weis E, et al. Initial evaluation of advanced collapsed cone engine dose calculations in water medium for ^{125}I seeds and COMS eye plaques. *Medical Physics*. 2018;**45**(3):1276-1286. DOI: 10.1002/mp.12776
- [12] de la Zerda A, Chiu-Tsao S, Lin J, Boulay LL, Kanna I, Tsao H. ^{125}I plaque dose distribution including penumbra characteristics. *Medical Physics*. 1996;**23**:407-418. DOI: 10.1118/1.597803
- [13] Saidi P, Sadeghi M, Shirazi A, Tenreiro C. Monte Carlo calculation of dosimetry parameters for the $\text{IR08-}^{103}\text{Pd}$ brachytherapy source. *Medical Physics*. 2010;**37**:2509-2515. DOI: 10.1118/1.3416922
- [14] Melhus CS, Rivard MJ. COMS eye plaque brachytherapy dosimetry simulations for ^{103}Pd , ^{125}I , and ^{131}Cs . *Medical Physics*. 2008;**35**:3364-3371. DOI: 10.1118/1.2940604
- [15] Saidi P, Sadeghi M, Tenreiro C. Experimental measurements and Monte

- Carlo calculations for $^{103}\text{-Pd}$ dosimetry of the 12 mm COMS eye plaque. *Physica Medica*. 2013;**29**:286-294. DOI: 10.1016/j.ejmp.2012.04.002
- [16] Chiu-Tsao ST, Astrahan MA, Finger PT, Followill DS, Meigooni AS, Melhus CS, et al. Dosimetry of 125I and $^{103}\text{-Pd}$ COMS eye plaques for intraocular tumors: Report of task group 129 by the AAPM and ABS. *Medical Physics*. 2012;**39**:6161-6184. DOI: 10.1118/1.4749933
- [17] Thomson RM, Rogers DWO. Monte Carlo dosimetry for 125I and $^{103}\text{-Pd}$ eye plaque brachytherapy with various seed models. *Medical Physics*. 2010;**37**:368-376. DOI: 10.1118/1.3271104
- [18] Rivard MJ, Coursey BM, DeWerd LA, Hanson WF, Huq MS, Ibbott GS, et al. Update of AAPM task group no. 43 report: A revised AAPM protocol for brachytherapy dose calculations. *Medical Physics*. 2004;**31**:633-674. DOI: 10.1118/1.1646040
- [19] Lesperance M, Inglis-Whalen M, Thomson RM. Model-based dose calculations for COMS eye plaque brachytherapy using an anatomically realistic eye phantom. *Medical Physics*. 2014;**41**(2):021717. DOI: 10.1118/1.4861715
- [20] Monte Carlo Team. MCNP-A General Monte Carlo N-Particle Transport Code-Version 5. Los Alamos National Laboratory; Available from: <http://mcnp-green.lanl.gov/index.html> [Accessed: 29 January 2004]
- [21] Sadeghi M, Tenreiro C, van den Winkel P. Study of heat transfer parameters on rhodium target for $^{103}\text{-Pd}$ production. *Nukleonika*. 2009;**54**:169-173
- [22] Saidi P, Sadeghi M, Enferadi M, Aslani GH. Investigation of palladium-103 production and IR07- $^{103}\text{-Pd}$ brachytherapy seed preparation. *Annals of Nuclear Energy*. 2011;**38**:2168-2173. DOI: 10.1016/j.anucene.2011.06.018
- [23] Saidi P, Sadeghi M, Hosseini SH. Thermoluminescent dosimetry of the IR06- $^{103}\text{-Pd}$ brachytherapy source. *Journal of Applied Clinical Medical Physics*. 2011;**12**(4):286-295. DOI: 10.1120/jacmp.v12i4.3581
- [24] Sadeghi M, Saidi P, Tenreiro C. Dosimetric characteristics of the brachytherapy sources based on Monte Carlo method. In: Mode CJ, editor. *Applications of Monte Carlo Methods in Biology, Medicine and Other Fields of Science*. Intech; 2011. pp. 155-176. DOI: 10.5772/15884
- [25] Sadeghi M, Farshadi A, Saidi P, Hosseini SH, Jafari A. Monte Carlo dosimetry for 125-I eye plaque brachytherapy. *Journal of Nuclear Medicine and Radiation Therapy*. 2018;**9**(4):1000367. DOI: 10.4172/2155-9619.1000367.
- [26] Williamson JF. Monte Carlo modeling of the transverse-axis dose distribution of the model 200 ^{103}Pd interstitial brachytherapy source. *Medical Physics*. 2000;**27**:643-654
- [27] Thomson RM, Taylor REP, Rogers DWO. Monte Carlo dosimetry for 125I and $^{103}\text{-Pd}$ eye plaque brachytherapy. *Medical Physics*. 2008;**35**:5530-5543. DOI: 10.1118/1.3002412
- [28] ICRU. Photon, Electron, Photon and Neutron Interaction Data for Body Tissues. ICRU Report 46; Washington D.C.: ICRU; 1992
- [29] Saidi P, Sadeghi M, Tenreiro C. Theory and applications of Monte Carlo simulations. In: Chan WKV, editor. *Variance Reduction of Monte Carlo Simulation in Nuclear Engineering Field*. Intech; 2013. pp. 153-172. DOI: 10.5772/53384., 2013
- [30] Meigooni AS, Bharucha Z, Yoe-Sein M, Sowards K. Dosimetric characteristic of the best double-wall $^{103}\text{-Pd}$ brachytherapy source. *Medical Physics*.

2001;**28**:2568-2575. DOI: 10.1118/
1.1414007

[31] Bearden JA, Burr AF. Reevaluation of X-ray atomic energy levels. *Medical Physics*. 1967;**39**:125-142. DOI: 10.1103

[32] Nath R, Yue N, Shahnazi K, Bongiorno PJ. Measurement of dose-rate constant for ^{103}Pd seeds with air kerma strength calibration based upon a primary national standard. *Medical Physics*. 2000;**27**:655-658. DOI: 10.1118/
1.598925

[33] Wallace RE, Fan JJ. Dosimetric characterization of a new design 103-palladium brachytherapy source. *Medical Physics*. 1999;**26**:2465-2470. DOI: 10.1118/1.598765

[34] Li Z, Palta JR, Fan JJ. Monte Carlo calculations and experimental measurements of dosimetry parameters of a new ^{103}Pd source. *Medical Physics*. 2000;**27**:1108-1112. DOI: 10.1118/
1.598975